JACS
JOURNAL OF THE AMERICAN CHEMICAL SOCIETY
Article
pubs.acs.org/JACS

Synthesis, Structure, and Magnetism of an f Element Nitrosyl Complex, $(C_5Me_4H)_3UNO$

Nathan A. Siladke,[a] Katie R. Meihaus,[b] Joseph W. Ziller,[a] Ming Fang,[a] Filipp Furche,*[,a] Jeffrey R. Long,*[,b] and William J. Evans*[,a]

[a]Department of Chemistry, University of California, Irvine, California 92627-2025, United States
[b]Department of Chemistry, University of California, Berkeley, California 94720-1460, United States

Supporting Information

ABSTRACT: $(C_5Me_4H)_3U$, **1**, reacts with 1 equiv of NO to form the first f element nitrosyl complex $(C_5Me_4H)_3UNO$, **2**. X-ray crystallography revealed a 180° U−N−O bond angle, typical for $(NO)^{1+}$ complexes. However, **2** has a 1.231(5) Å N═O distance in the range for $(NO)^{1-}$ complexes and a short 2.013(4) Å U−N bond like the U═N bond of uranium imido complexes. Structural, spectroscopic, and magnetic data as well as DFT calculations suggest that reduction of NO by U^{3+} has occurred to form a U^{4+} complex of $(NO)^{1-}$ that has π interactions between uranium 5f orbitals and NO π^* orbitals. These bonding interactions account for the linear geometry and short U−N bond. The complex displays temperature-independent paramagnetism with a magnetic moment of 1.36 μ_B at room temperature. Complex **2** reacts with Al_2Me_6 to form the adduct $(C_5Me_4H)_3UNO(AlMe_3)$, **3**.

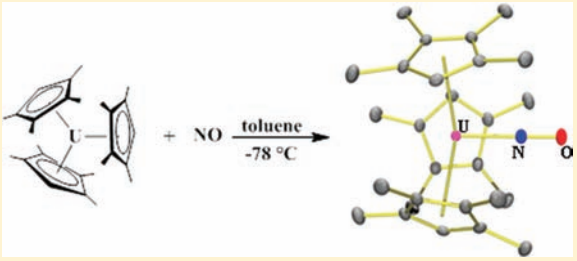

INTRODUCTION

The recent synthesis of an $(NO)^{2-}$ complex of yttrium, $\{[(Me_3Si)_2N]_2Y(THF)\}_2(\mu-\eta^2:\eta^2\text{-NO})$,[1] eq 1, highlighted the fact that there are no known complexes of the more common $(NO)^{1-}$and $(NO)^{1+}$ ligands with rare earth and actinide metals. A review on organometallic NO chemistry states that complexes of the electropositive metals are rare due to the oxophilic nature of these metals and the oxidizing power of NO.[2] Indeed, reactions of NO with lanthanides[3] and actinides[4,5] have formed oxide, not nitrosyl products, eqs 2 and 3.

Since uranium is known to bind analogs of $(NO)^{1+}$, such as CO[6−12] and N_2,[11,13] as well as analogs of $(NO)^{1-}$, a pseudohalide, it seemed that uranium should also be capable of binding NO.[14] However, bimetallic oxide forming reactions such as eq 3 would have to be avoided.

The coordination environments provided by tris(polyalkylcyclopentadienyl) complexes such as $(C_5Me_5)_3U$[15] and $(C_5Me_4H)_3U$[6,8,16] seemed to be attractive for these purposes. If all three cyclopentadienyl ligands remained η^5 in the product, the complex would be too crowded to form bimetallic oxide species like the products shown in eqs 2 and 3. In addition, although an extensive uranium CO chemistry is developing,[9,11,12,17−19] the few uranium CO adducts that have been stable enough to characterize crystallographically were found with the tris(polyalkylcyclopentadienyl) uranium complexes $(C_5Me_5)_3U$[7] and $(C_5Me_4H)_3U$.[6,8] Further support for this approach arises from Meyer's successful binding of CO_2 to uranium[20] using a ligand system that provides a 3-fold symmetric cavity with a single pocket for reactivity.[21] Since $(C_5Me_5)_3U$[7] and $(C_5Me_4H)_3U$[6,8] both form CO adducts, $(C_5Me_5)_3U(CO)$[7] and $(C_5Me_4H)_3U(CO)$,[6,8] and halide complexes, for example, $(C_5Me_5)_3UCl$[16] and $(C_5Me_4H)_3UCl$,[6,8,16] respectively, they were investigated for their potential to stabilize NO. The existence of tris(cyclopentadienyl) uranium nitrosyls has been predicted theoretically by Bursten et al. since 1989.[22] Xα calculations performed on $(C_5H_5)_3UNO$ indicated that this complex could have a linear U−N−O linkage due to π bonding between the metal and NO ligand and could also be diamagnetic.[22]

We report here the reactivity of NO with $(C_5Me_4H)_3U$ and the closely related $(C_5Me_5)_3U$ and $(C_5Me_4SiMe_3)_3U$, the isolation of the first f element nitrosyl complex, and the reactivity of this complex with a Lewis acid.

EXPERIMENTAL SECTION

The syntheses and manipulations described below were conducted under argon or nitrogen with rigorous exclusion of air and water using glovebox, Schlenk, and vacuum-line techniques. The argon glovebox was free of coordinating solvents unless otherwise noted. Solvents were sparged with argon and dried over columns containing Q-5 and 4A molecular sieves. Toluene-d_8 was dried over sodium−potassium alloy, degassed using three freeze−pump−thaw cycles, and vacuum transferred before use. UI_3,[23] KC_5Me_4H,[16] $(C_5Me_4H)_3UCl$,[24] and $(C_5Me_4H)_3U$,[16] **1**, were prepared according to the literature. NO gas was purchased from Aldrich (98.5%), and passed through two U-shaped glass columns connected in series and cooled to −78 °C. ^{15}NO was purchased from Cambridge Isotopes Laboratories and purified similarly. Al_2Me_6 was purchased from Aldrich and used as received. NMR spectra were recorded with a Bruker DRX 500 MHz

Received: October 12, 2011
Published: December 2, 2011

   dx.doi.org/10.1021/ja2096128 | J. Am. Chem.Soc. 2012, 134, 1243−1249

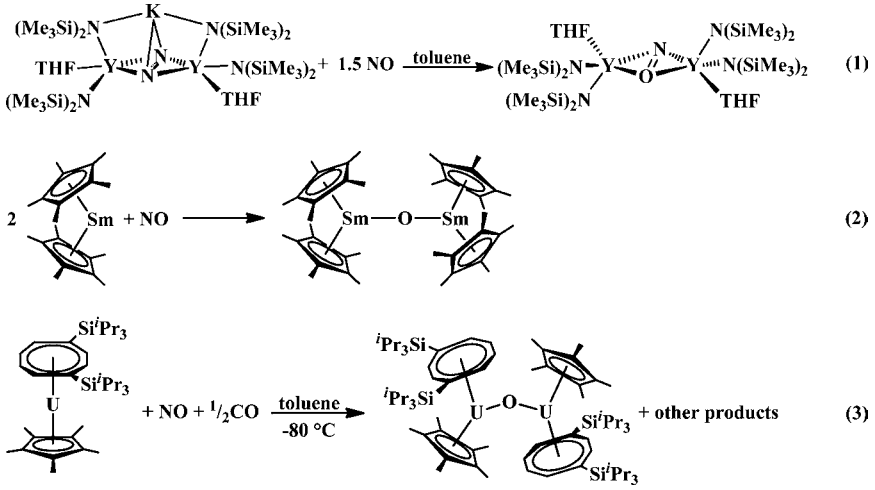

spectrometer. Due to the paramagnetism of uranium, only resonances that could be unambiguously identified are reported. Infrared spectra were recorded as KBr pellets on a Varian 1000 FT-IR spectrometer. Elemental analysis was performed on a Perkin-Elmer 2400 Series II CHNS analyzer. Electronic absorption measurements were made in toluene using a Perkin-Elmer Lambda 900 UV/vis/NIR spectrometer in a 1 cm quartz cell attached to a greaseless high vacuum stopcock. APCI-MS spectra were obtained on a Waters (Micromass) LCT Premier orthogonal time-of-flight mass spectrometer using toluene as the solvent and the reagent ion source. Each analyte/toluene solution was loaded in a syringe in the glovebox. The needle was sealed with a rubber septum and analysis was performed immediately after removing the syringe from the glovebox.

The magnetic susceptibility samples were prepared by adding 131.3 mg (**2**) or 104.5 mg ($(C_5Me_4H)_3UCl$) of crystalline compound, crushed to a fine powder, to a 7 mm quartz tube with raised quartz platform. Sufficient liquid eicosane (heated at 60 °C) was added to saturate and cover the sample to prevent crystallite torquing and provide good thermal contact between the sample and the bath. The tube was fitted with a Teflon sealable adapter, evacuated using a glovebox vacuum pump, and sealed with an H_2/O_2 flame under vacuum.

Magnetic susceptibility measurements were collected using a Quantum Design MPMS2 SQUID magnetometer. Dc susceptibility data measurements were performed at temperatures ranging from 1.8 to 300 K and applied fields of 1000, 5000, and 10000 Oe. Magnetization data for **2** was collected at 100 K with the field ranging from 0 to 70000 Oe. All data for **2** and $(C_5Me_4H)_3UCl$ were corrected for diamagnetic contributions from the core diamagnetism estimated using Pascal's constants to give $\chi_D = -0.00032844$ emu/mol for **2** and $\chi_D = -0.00034427$ for $(C_5Me_4H)_3UCl$.

$(C_5Me_4H)_3UNO$, 2. A 100 mL side arm Schlenk flask equipped with a Teflon stopcock containing a green/brown solution of $(C_5Me_4H)_3U$, **1**, (0.216 g, 0.612 mmol) in toluene (15 mL) was connected to a glass T-joint on a high-vacuum line. The other end of the glass T-joint was attached to a 56 mL Schlenk flask equipped with a Teflon stopcock that was used to measure the amount of NO assuming ideal gas behavior. The toluene solution of **1** was degassed by three freeze–pump–thaw cycles and frozen in liquid N_2. NO gas was then slowly introduced to the 56 mL Schlenk flask to a pressure of 59 mmHg. The Teflon stopcock of the 56 mL Schlenk flask was then closed and the system evacuated under high vacuum. The NO gas was then condensed into the flask containing **1** (about 5 min). The reaction flask was sealed and the liquid N_2 bath was removed and immediately replaced with a dry ice/acetone bath. The mixture of **1** and NO was allowed to stir for 1 h at −78 °C before the reaction was allowed to warm up to room temperature. During this time, the color of the solution turned to red/brown. The reaction flask was then brought into a glovebox and the solvent removed under vacuum to yield a dark brown microcrystalline solid. This solid was dissolved in a minimal amount of toluene (8 mL) and placed into a freezer at −35 °C to yield dark-brown crystals of $(C_5Me_4H)_3UNO$, **2**, from which three crops of crystals were collected and combined (0.140 g, 62%). After collecting the crystal crops, ^{1}H NMR of the mother liquor showed remaining **2**, along with impurities, which could not be recovered. Single crystals suitable for X-ray analysis were grown from a concentrated solution of toluene at −35 °C. ^{1}H NMR (toluene-d_8, −45 °C): δ 3.9 (s, $\Delta\nu_{1/2}$ = 4 Hz, 9H, C_5Me_4H), 4.9 (s, $\Delta\nu_{1/2}$ = 5 Hz, 9H, C_5Me_4H), 5.1 (s, $\Delta\nu_{1/2}$ = 4 Hz, 9H, C_5Me_4H), 8.9 (s, $\Delta\nu_{1/2}$ = 4 Hz, 9H, C_5Me_4H), 11.6 (s, $\Delta\nu_{1/2}$ = 3 Hz, 3H, C_5Me_4H). Due to the low solubility of **2** in toluene-d_8 at the −45 °C temperature for the ^{1}H NMR spectrum, ^{13}C NMR data were not obtained. IR: 2904s, 2861s, 1439vs, 1373vs, 1020 m, 792 m, 760w, 600w cm^{-1}. Anal. Calcd for $C_{27}H_{39}NOU$: C, 51.34; H, 6.22; N, 2.22. Found: C, 51.81; H, 6.28; N, 1.89. MS (APCI, toluene) m/z (rel intensity): 632.4 (30) $[(C_5Me_4H)_3UNOH]^+$, 601.4 (100) $(C_5Me_4H)_3U$. NIR (3.0 mmol, toluene): 6200 (ε = 320 M^{-1} cm^{-1}), 8800 (ε = 180 M^{-1} cm^{-1}), and 14400 cm^{-1} (ε = 260 M^{-1} cm^{-1}). Complex **2** is stable at room temperature and under vacuum and is soluble in alkane and arene solvents.

$(C_5Me_4H)_3U^{15}NO$, 2-^{15}NO. This complex was prepared as described for **2** but using ^{15}N-enriched NO. The purity of **2-^{15}NO** was confirmed by ^{1}H NMR spectroscopy and mass spectrometry. IR: 1416vs, 1366vs cm^{-1}. MS (APCI, toluene) m/z (rel intensity): 633.4 (40) $[(C_5Me_4H)_3U^{15}NOH]^+$, 601.4 (100) $(C_5Me_4H)_3U$.

$(C_5Me_4H)_3UNO(AlMe_3)$, 3. Al_2Me_6 (12 μL, 0.06 mmol) was added to a stirred solution of **2** (0.077 g, 0.12 mmol) in toluene (10 mL). The red/brown solution immediately became more intensely red and the solution was allowed to stir for 30 min. The solvent was removed under vacuum to yield a dark-brown powder (0.084 g, 99%). ^{1}H NMR (toluene-d_8, −55 °C): δ −1.3 (s, $\Delta\nu_{1/2}$ = 3 Hz, 9H, $AlMe_3$), 3.9 (bs, $\Delta\nu_{1/2}$ = 36 Hz, 3H, C_5Me_4H), 4.8 (s, $\Delta\nu_{1/2}$ = 11 Hz, 9H, C_5Me_4H), 5.0 (s, $\Delta\nu_{1/2}$ = 5 Hz, 9H, C_5Me_4H), 6.0 (s, $\Delta\nu_{1/2}$ = 14 Hz, 9H, C_5Me_4H), 7.5 (s, $\Delta\nu_{1/2}$ = 11 Hz, 9H, C_5Me_4H). Due to the low solubility of **3** in toluene-d_8 at the −55 °C temperature for the ^{1}H NMR spectrum, ^{13}C NMR data were not obtained. IR: 2913s, 2880 m, 1440 m, 1373 m, 1303vs, 1167 m, 1109w, 1020 m, 813 m, 679vs, 612 m, 533 m cm^{-1}. Anal. Calcd for $C_{30}H_{48}NOAlU$: C, 51.20; H, 6.88; N, 1.99. Found: C, 51.26; H, 6.87; N, 1.95.

$(C_5Me_4H)_3U^{15}NO(AlMe_3)$, 3-^{15}NO. This complex was prepared analogously to **3**, but using **2-^{15}NO**. ^{1}H NMR spectroscopy was used to confirm the purity of the sample. IR: 1430 m, 1280vs cm^{-1} (1279 cm^{-1} calculated).

X-ray Crystallography Data Collection. Detailed information on the X-ray data collection, structure determination, and refinement for **2**, as well as the unit cell data collected for **3**, are provided in the Supporting Information.

■ COMPUTATIONAL DETAILS

The structure of **2** was initially optimized using the TPSS[25] meta-GGA functional and TPSSh[26] hybrid meta-GGA functional and split valence

basis sets with polarization functions on non-hydrogen atoms (SV(P)).[27] TPSS and TPSSh were chosen due to their established performance for transition metal compounds with partially filled open shells.[28−30] Relativistic small-core pseudopotentials[31] were employed for uranium. Fine quadrature grids (size m4)[32] were used throughout. The multipole-accelerated resolution of the identity (MARI-J) approximation for the Coulomb energy was used throughout.[33] Vibrational frequencies were computed at the TPSS/TPSSh/SV(P)[34] level and scaled by a factor of 0.95 to account for anharmonicity and basis set incompleteness.[1,35] All structures were found to be minima. Natural population analyses[36] were obtained at the TPSS/TPSSh/SV(P) level; the contour values were 0.08 for orbital plots. The structural parameters reported in the text are the result of reoptimization using larger triple-ζ valence basis sets with two sets of polarization functions (def2-TZVP, except for U, in which case def-TZVP was used).[37] The differences between the SV(P) and the TZVP structures were found to be small, typically amounting to 0.01 Å in bond lengths or less. All computations were performed using the TURBOMOLE program package.[38]

RESULTS AND DISCUSSION

Synthesis. Exposure of toluene solutions of the sterically crowded complexes $(C_5Me_5)_3U$[15] and $(C_5Me_4SiMe_3)_3U$[39] to stoichiometric amounts of NO on a vacuum line at −78 °C for 1 h led to complicated reaction mixtures from which pure crystalline products have not yet been obtained. On the other hand, green/brown toluene solutions of the sterically less demanding $(C_5Me_4H)_3U$, **1**, react with one equiv of NO at −78 °C over 1 h to form a red/brown solution from which dark brown crystalline **2** can be isolated. Compound **2** was identified as $(C_5Me_4H)_3UNO$, eq 4, based on spectroscopy, elemental

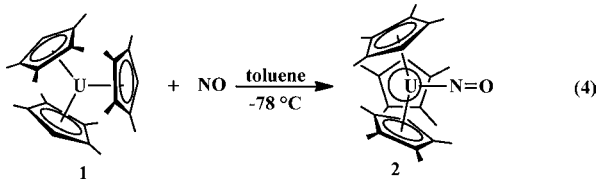

(4)

analysis, and X-ray crystallography, Figure 1. The reaction of **1** with excess NO yields a complicated mixture that does not contain **2** by ^{1}H NMR spectroscopy.

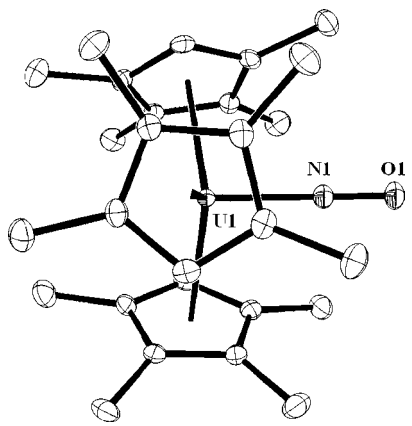

Figure 1. Thermal ellipsoid plot of $(C_5Me_4H)_3UNO$, **2**, drawn at the 50% probability level with hydrogen atoms omitted for clarity. Selected bond distances (Å) and angles (deg) for **2**: U1−(ring centroid) 2.491, U1−N1 2.013(4), N1−O1 1.231(5), (ring centroid)−U1−(ring centroid) 118.8, (Cnt)−U1−N1 96.5, U1−N1−O1 180.0(4).

NMR Spectroscopy. The room temperature ^{1}H NMR spectrum of **2** contains broad ($\Delta\nu_{1/2}$ = 5 to 2650 Hz) and overlapping resonances. The resonances sharpen upon cooling and at −45 °C, four resonances integrating to 9H and one integrating to 3H are resolvable. This is consistent with the solid state structure of **2**, Figure 1, in which the three $(C_5Me_4H)^{1-}$ rings are equivalent and each methyl group is unique. Similar spectra have been reported for $(C_5Me_4H)_3UCl$[24] and $(C_5Me_4H)_3UI$.[16] These observations suggest that the structure of **2** is fluxional in solution at room temperature.

X-ray Crystal Structure. Complex **2** has a distorted tetrahedral geometry similar to previously reported $(C_5Me_4H)_3UQ$ complexes, where Q is either an anionic or a neutral donor ligand.[6,8,16,24,40] Table 1 shows that the U−(ring centroid) distance for **2** is the shortest of all the $(C_5Me_4H)_3UQ$ complexes, but there is overlap in this parameter for U^{4+} and U^{3+} complexes such that it cannot be used to specify oxidation state as is common in rare earth complexes. This has been noted before for uranium $(C_5Me_5)^{1-}$ complexes.[41]

The U−N−O bond angle is linear at 180.0(4)°, which is typically observed for metal complexes containing an $(NO)^{1+}$ ligand.[42] However, the 1.231(5) Å N−O bond distance in **2** is closer to the 1.26 Å double bond distance typically found in $(NO)^{1-}$ complexes than to the 1.06 Å triple bond distance found in $(NO)^{1+}$ compounds.[43] The 2.013(4) Å U−N bond distance is significantly shorter than U−N single bonds, which are typically 2.18 to 2.25 Å for U^{4+} complexes[44] and 2.23 to 2.43 Å for U^{3+} compounds.[45−49] This short U−N bond distance in **2** is similar to U=N uranium imido bonds in U^{4+} complexes, which range from 1.952(12) to 2.097(5) Å.[50−53]

IR and NIR Spectroscopy. The IR spectrum of **2** contains no absorptions in the ∼1700 cm^{-1} region expected for linear $(NO)^{1+}$ complexes.[43] In fact, no absorption in the spectrum stands out as a likely N−O stretch. The IR spectrum of $(C_5Me_4H)_3U^{15}NO$, **2-^{15}NO**, prepared from ^{15}NO, showed shifts of the absorptions at 1439 and 1373 cm^{-1} in **2** to 1416 and 1366 cm^{-1} in **2-^{15}NO**. These shifts suggest that the NO stretch is obscured by $(C_5Me_4H)^{1-}$ ligand absorptions. This low N−O stretch is consistent with the N=O double bond distance observed in **2**, the ∼1470 cm^{-1} absorptions typically observed for $(NO)^{1-}$ complexes,[43] and the DFT calculations described below.

The near-infrared (NIR) spectrum of **2**, Figure S1 (Supporting Information), contains broad absorptions with ε values of 180−320 M^{-1} cm^{-1}. These extinction coefficients as well as the spectral shape are typical of U^{4+} complexes with strongly interacting ligands such as ketimide and imido ligands.[54] In contrast, structurally similar $(C_5Me_5)_3UMe$[55] has sharp transitions with smaller ε values (30−130 M^{-1} cm^{-1}) typical of complexes having simple σ bonding ligands.[54]

Magnetic Susceptibility. Room temperature magnetic moment measurements by the Evans[56] method gave a magnetic moment of 1.4 μ_B for **2**, which is low compared to room temperature values typical for both U^{4+} and U^{3+} complexes.[48,57−59] Variable temperature magnetic susceptibility measurements were made to examine the magnetism of **2** in more detail. $(C_5Me_4H)_3UCl$[24] was also examined for comparison since it is an analog with a simple chloride ligand instead of nitrosyl. $(C_5Me_4H)_3UCO$ has previously been reported to display Curie−Weiss behavior between 0 and −70 °C.[6] Figure 2 is a plot of $\chi_M T$ versus T for **2** (red circles) and $(C_5Me_4H)_3UCl$ (blue squares). The susceptibility of

dx.doi.org/10.1021/ja2096128 | J. Am. Chem.Soc. 2012, 134, 1243−1249

Table 1. Comparison of $(C_5Me_4H)_3UQ$ Structural Parameters

complex	formal U oxidation state	U−Q (Å)	Cnt−U (Å)	Cnt−U−Cnt (deg)	Cnt−U−Q (deg)
$(C_5Me_4H)_3U$[6,8]	3+	N/A	2.523	120.0	N/A
$(C_5Me_4H)_3UCO$[6,8]	3+	2.383(6)	2.531	118.8−120.0	95.53
$(C_5Me_4H)_3U(THF)$[40]	3+	2.650(6)	2.597	116.8	100.4
$(C_5Me_4H)_3U(CNC_6H_4$-p-$OMe)$[6]	3+	2.464(4)	2.554	119.6	98.49
$(C_5Me_4H)_3UCl$[24]	4+	2.637	2.520	117.9	98.4
$(C_5Me_4H)_3UI$[16]	4+	3.0338(5)	2.524	117.5	99.2
$(C_5Me_4H)_3UNO$[a]	4+	2.013(4)	2.491	118.8	96.5

[a]Reported here.

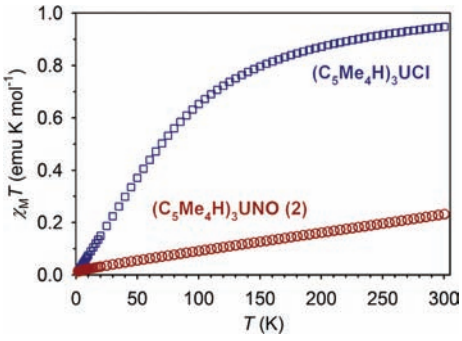

Figure 2. Plot of the temperature dependence of $\chi_M T$ for **2** and $(C_5Me_4H)_3UCl$ from 1.8 to 300 K collected at an applied field of 1000 Oe.

$(C_5Me_4H)_3UCl$ is typical for a U^{4+} species[58] with a $\chi_M T$ value of 0.947 emu K mol^{-1} at 300 K that corresponds to a room temperature magnetic moment of μ_{eff} = 2.75 μ_B. This value drops off gradually with decreasing temperature due to depopulation of thermally accessible anisotropic excited states. Below 50 K, the susceptibility becomes temperature independent (Figure S3, blue squares, Supporting Information) revealing that no excited states are thermally accessible at these lower temperatures. The values of $\chi_M T$ tends toward zero with a minimum value of 0.014 emu K mol^{-1} (μ_{eff} = 0.33 μ_B) at 1.8 K demonstrating the anticipated singlet ground state for a U^{4+} complex.

Complex **2** exhibits drastically different magnetic behavior from $(C_5Me_4H)_3UCl$. Most notable is the linear decline of $\chi_M T$ that is the result of temperature-independent paramagnetism (TIP). The room temperature $\chi_M T$ value of 0.232 emu K mol^{-1} for **2** is much lower than that of $(C_5Me_4H)_3UCl$ and corresponds to a magnetic moment of 1.36 μ_B that is in good agreement with the measurement done by the Evans method. At 1.8 K, $\chi_M T$ has dropped to a value of 0.014 emu K mol^{-1} (μ_{eff} = 0.33 μ_B) which indicates a singlet ground state. The TIP (χ_{TIP} = 7.7 × 10^{-4} emu K mol^{-1} at 300 K) dictates the susceptibility and ultimately leads to the lower than anticipated room temperature magnetic moment.[60] Temperature-independent susceptibility over such a wide range has been observed previously for U^{4+} in octahedral tetrahalide systems incorporating strongly donating amide, phosphine oxide, and arsine oxide ligands.[61,62] In the absence of thermally accessible excited states, the observed paramagnetic susceptibility arises from field-induced mixing of the ground state with a higher-spin excited state. For **2**, the persistence of linearity in $\chi_M T$ versus T as high as 340 K (Figure S4, Supporting Information) reveals that, even at this temperature, excited states remain thermally inaccessible, and the observed susceptibility can be ascribed to field-induced mixing of the singlet ground state with a paramagnetic excited state. Assuming that an excited state population of 5% or greater would be necessary to observe temperature dependence in the magnetic susceptibility, a rough estimate of the energy gap between the ground and an excited triplet state can be obtained. Supposing an excited state population of no greater than 4% at 340 K, one calculates from Boltzmann statistics a lower bound of 700 cm^{-1} for the separation between the two states.

Theoretical Studies. Density functional theory calculations were performed on **2** to help explain the data. The Tao−Perdew−Staroverov−Scuseria (TPSS)[25] functional and its hybrid analog (TPSSh) were used starting from the

Table 2. Experimental and Computed Bond Distances and Frequencies and Computed Energies for 2

	functional	energy (Hartree)	U−N (Å)	N−O (Å)	U−Cp(cnt) (Å)	ν(N−O) cm^{-1}
Exp			**2.013(4)**	**1.231(5)**	**2.491 (C3)**	**1439**
Triplet	TPSSh	−1658.36649	2.095	1.203	2.514	1540
					2.525	
					2.524	
	TPSS	−1658.49956	2.085	1.214	2.515	1499
					2.527	
					2.525	
Singlet	TPSSh	−1658.36345	1.960	1.226	2.499 (C3)[a]	1480
	TPSS	−1658.49955	1.978	1.235	2.507	1445
					2.507	
					2.508	
Quintet	TPSSh	−1658.35977	2.219	1.196	2.520	1639
					2.521	
					2.605	

[a]C1 symmetry was used as a starting point for the geometry optimization and the final symmetry after optimization was C3.

dx.doi.org/10.1021/ja2096128 | J. Am. Chem.Soc. 2012, 134, 1243−1249

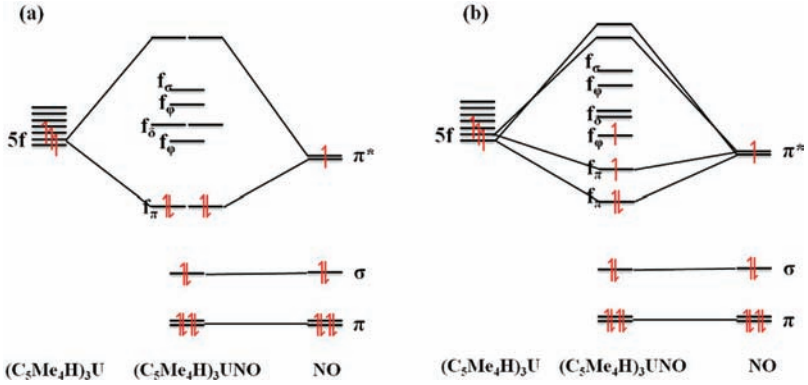

Figure 3. Simplified molecular orbital scheme of **2**: (a) singlet, (b) triplet.

experimentally determined structural parameters.[26] Structures for three possible spin states, that is, singlet, triplet, and quintet, were optimized. The energetic separation of the singlet and triplet states was found to be less than 2 kcal/mol (700 cm^{-1}), with TPSS slightly favoring the singlet and TPSSh slightly favoring the triplet state, while the quintet state was computed to be 4 kcal/mol higher in energy. Thus, the singlet and triplet states are isoenergetic within the accuracy of these methods. The magnetic susceptibility measurements, however, confirm that the singlet is the ground state and the details of the TIP indicate that a paramagnetic excited state exists that leads to the observed magnetic moment.[60]

Both of the singlet and triplet calculations showed good agreement in bond distances, Table 2, and N−O stretching frequencies with the experimental data. Those from the singlet calculations matched slightly better, but either calculation could explain the linear U−N−O linkage and the short U−N bond as described below. Calculations on the O-bonded isomer, $(C_5Me_4H)_3UON$, a structure that is conceivable due to the oxophility of uranium, indicated that this structure was 22.8 kcal/mol higher in energy.

The following theoretical results were obtained using the TPSS functional unless otherwise stated. Frequency calculations on **2** predict a strong N−O stretching absorption at 1445 cm^{-1} (singlet ground state, Table 2 and Figure S2, Supporting Information) or 1499 cm^{-1} (triplet ground state, Table 2). These values are close to the absorptions predicted from C═C ring stretching and C−H bending modes in **2**. This is consistent with the experimental spectra of **2** and **2-^{15}NO** in which overlap of other absorptions prevented definitive assignment of an NO stretch. Interestingly, DFT shows that this N−O stretching mode in **2** is strongly coupled to the C−H bending modes of CH_3 groups on the $(C_5Me_4H)^{1-}$ rings. The calculated values can be compared to a typical $(NO)^{1-}$ compound such as HNO which has an N−O stretch[63] at 1371 cm^{-1} and neutral NO which has an N−O stretch at 1918 cm^{-1}.[43] The fact that the N−O stretching frequency for **2** is close to that in HNO is consistent with the $U^{4+}/(NO)^{1-}$ assignment.

Inspection of the computed Kohn−Sham molecular orbitals explains the observed short U−N distance and linear U−N−O angles in both the singlet and triplet models. Figure 3 shows simplified molecular orbital diagrams for the singlet and triplet states. In both the singlet state, with a formal $(C_5Me_4H)_3U{\equiv}N^+{-}O^-$ zwitterionic structure, and the triplet state, with a $U^{4+}/(NO)^{1-}$ $(C_5Me_4H)_3U{-}N{=}O$ structure, the two orthogonal π^* orbitals of NO interact strongly with the two 5f orbitals that have π symmetry. In the singlet case (Figures 3a and 4), **2** adopts C_3 symmetry with a doubly degenerate highest occupied

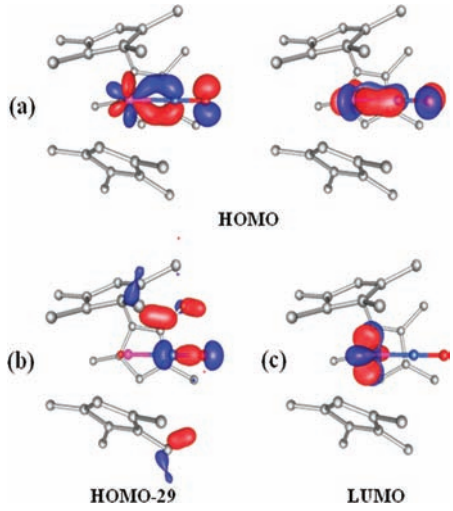

Figure 4. DFT results on **2** (singlet): (a) two degenerate HOMOs showing the 5f to NO π^* interaction, (b) HOMO-29 showing the weak dative interaction of the NO σ lone pair, and (c) the LUMO which is one of the nonbonding f_φ orbitals (all contour values are 0.08).

molecular orbital (HOMO) formed from π interactions between the two symmetry equivalent $5f_\pi$ orbitals and the two NO π^* orbitals. This singlet state molecular orbital diagram is in accord with the one presented previously by Bursten et al..[22] Natural population analysis (NPA) showed that this degenerate HOMO has 49% uranium 5f character and 35% NO π^* character. Since the nitrogen lone pair of NO is contracted and low in energy, it only forms a weak dative interaction with uranium (HOMO-29, Figure 4b). The lowest unoccupied molecular orbital (LUMO) of **2** is a nonbonding $5f_\varphi$ orbital.

In the triplet state, Jahn−Teller distortion can occur to lower the symmetry from C_3 to C_1 and the $5f_\pi$ orbitals are no longer degenerate in this case (Figures 3b and 5). Only one forms a doubly occupied molecular orbital with π bonding to NO. The other $5f_\pi$ orbital is also π bonding, but it is only singly occupied. This other $5f_\pi$ orbital and the $5f_\varphi$ (the LUMO in the singlet picture) are singly occupied and account for the $5f^2$ U^{4+} configuration. However, the geometric distortion from C_3 symmetry is small (see Table 2), and the U−N−O unit remains nearly linear in the triplet state with a U−N−O angle

dx.doi.org/10.1021/ja2096128 | J. Am. Chem.Soc. 2012, 134, 1243−1249

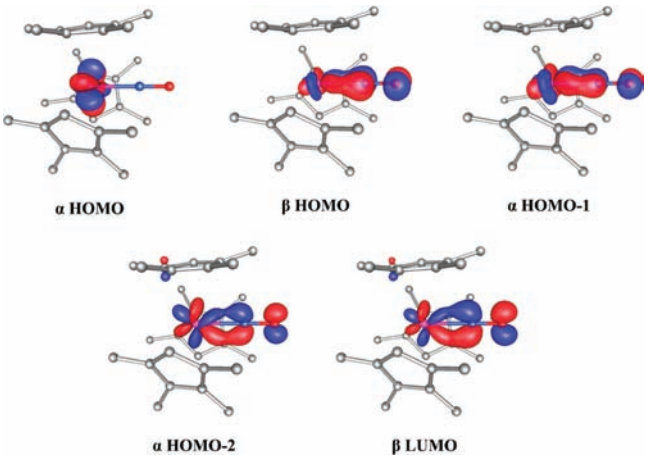

Figure 5. Molecular orbital plots of **2** in the triplet state showing the 5f to NO π^* interaction. Drawn with a contour value of 0.08.

of 179.3°. The U−N distance is only slightly elongated in the triplet state compared to the singlet structure. This is consistent with a reduction of the π bond order from 2 to 1.5 in the simplified model of Figure 3.

Reactivity. A well established mode of reactivity in transition metal nitrosyl complexes is the formation of Lewis acid adducts by coordination to the basic oxygen atom of the NO ligand.[2] As shown in Figure 4, the DFT calculations on **2** suggested that the HOMO has significant electron density on oxygen to make it Lewis basic. Although $B(C_6F_5)_3$, BPh_3, and 9-borabicyclo[3.3.1]nonane did not form isolable products, Al_2Me_6 cleanly reacts with **2** to form a complex formulated as $(C_5Me_4H)_3UNO(AlMe_3)$, **3**, eq 5, based on spectroscopic characterization and elemental analysis.

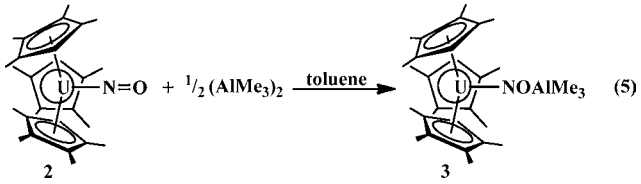

Like **2**, the room temperature ^1H NMR spectrum of **3** contained broad and overlapping resonances, but cooling to −55 °C gave four sharpened resonances integrating to 9H and one integrating to 3H for the ring protons, as well as a resonance of 9H attributable to $AlMe_3$. Crystallographic data on **3** were supportive but not definitive due to disorder in the atoms between the uranium and aluminum. On the other hand, the IR spectrum showed absorptions consistent with **3**. A strong absorbance at 1303 cm^{-1} was observed in addition to the signals in the IR spectrum of **2**. However, the absorptions in the 1450−1300 cm^{-1} region in the spectrum of **3** were less intense than those in **2**, which is consistent with the N−O stretch assignments for **2**. The 1303 cm^{-1} absorption is attributed to the N−O bond in **3** since it shifts to 1280 cm^{-1} (1279 cm^{-1} calculated) in $(C_5Me_4H)_3U^{15}NO(AlMe_3)$, **3-^{15}NO**, prepared from **2-^{15}NO**. N−O stretching frequencies are typically reduced as a result of coordination by a Lewis acid to a nitrosyl complex since the Lewis acid adduct drains electron density from an orbital that is bonding with respect to N and O.[2]

CONCLUSION

The coordination environment of $(C_5Me_4H)_3U$ has provided the first uranium nitrosyl complex, $(C_5Me_4H)_3UNO$, **2**. Moreover, it has led to a nitrogen oxide product that is unusual in structure, magnetism, and bonding. NO can be reduced by U^{3+} as originally postulated by Bursten.[22] The resulting ligand is formally $(NO)^{1-}$ with an N═O double bond, but strong interactions between the uranium $5f_\pi$ orbitals and the π^* orbitals of the NO ligand lead to a short U−N distance and linear U−N−O geometry. DFT and magnetic susceptibility studies suggest that the complex is best described with an electronic ground state that is a singlet having a formal $(C_5Me_4H)_3U{\equiv}N^+{-}O^-$ zwitterionic structure with a low-lying excited triplet state corresponding to the $U^{4+}/(NO)^{1-}$ structure $(C_5Me_4H)_3U{-}N{=}O$.

ASSOCIATED CONTENT

Supporting Information

Computational details and data, X-ray diffraction details of **2** and unit cell data collected for **3**, the NIR of **2**, and detailed magnetic data for **2** and $(C_5Me_4H)_3UCl$. This material is available free of charge via the Internet at http://pubs.acs.org. CCDC 832352 (**2**) contains the supplementary crystallographic data for this paper. These data can be obtained free of charge from The Cambridge Crystallographic Data Centre via www.ccdc.cam.ac.uk/data_request/cif.

AUTHOR INFORMATION

Corresponding Author

filipp.furche@uci.edu; jrlong@berkeley.edu; wevans@uci.edu

ACKNOWLEDGMENTS

We thank the Chemical Sciences, Geosciences, and Biosciences Division of the Office of Basic Energy Sciences of the Department of Energy and the U.S. National Science Foundation CHE-0840513 and CHE-1111900 for support. K.R.M. gratefully acknowledges the support of the NSF Graduate Research Fellowship Program. We also thank John Greaves for assistance with the mass spectrometry, Ryan Zarkesh for assistance with X-ray crystallography, and Bruce Bursten for helpful discussion.

REFERENCES

(1) Evans, W. J.; Fang, M.; Bates, J. E.; Furche, F.; Ziller, J. W.; Kiesz, M. D.; Zink, J. I. *Nature Chem.* **2010**, *2*, 644.
(2) Hayton, T. W.; Legzdins, P.; Sharp, W. B. *Chem. Rev.* **2002**, *102*, 935.
(3) Evans, W. J.; Grate, J. W.; Bloom, I.; Hunter, W. E.; Atwood, J. L. *J. Am. Chem. Soc.* **1985**, *107*, 405.
(4) Avens, L. R.; Barnhart, D. M.; Burns, C. J.; McKee, S. D.; Smith, W. H. *Inorg. Chem.* **1994**, *33*, 4245.
(5) Frey, A. S. P.; Cloke, F. G. N.; Coles, M. P.; Hitchcock, P. B. *Chem.—Eur. J.* **2010**, *16*, 9446.
(6) Conejo, M.; Parry, J. S.; Carmona, E.; Schultz, M.; Brennann, J. G.; Beshouri, S. M.; Andersen, R. A.; Rogers, R. D.; Coles, S.; Hursthouse, M. *Chem.—Eur. J.* **1999**, *5*, 3000.
(7) Evans, W. J.; Kozimor, S. A.; Nyce, G. W.; Ziller, J. W. *J. Am. Chem. Soc.* **2003**, *125*, 13831.
(8) Parry, J.; Carmona, E.; Coles, S.; Hursthouse, M. *J. Am. Chem. Soc.* **1995**, *117*, 2649.
(9) Frey, A. S.; Cloke, F. G. N.; Hitchcock, P. B.; Day, I. J.; Green, J. C.; Aitken, G. *J. Am. Chem. Soc.* **2008**, *130*, 13816.
(10) Castro-Rodriguez, I.; Meyer, K. *J. Am. Chem. Soc.* **2005**, *127*, 11242.

(11) Mansell, S. M.; Kaltsoyannis, N.; Arnold, P. L. *J. Am. Chem. Soc.* **2011**, *133*, 9036.
(12) Arnold, P. L.; Turner, Z. R.; Bellabarba, R. M.; Tooze, R. P. *Chem. Sci.* **2011**, *2*, 77.
(13) Fox, A. R.; Bart, S. C.; Meyer, K.; Cummins, C. C. *Nature* **2008**, *455*, 341.
(14) Arnold, P. L. *Chem. Commun.* **2011**, *47*, 9005.
(15) Evans, W. J.; Forrestal, K. J.; Ziller, J. W. *Angew. Chem., Int. Ed. Engl.* **1997**, *36*, 774.
(16) Evans, W. J.; Kozimor, S. A.; Ziller, J. W.; Fagin, A. A.; Bochkarev, M. N. *Inorg. Chem.* **2005**, *44*, 3993.
(17) Summerscales, O. T.; Cloke, F. G. N.; Hitchcock, P. B.; Green, J. C.; Hazari, N. *Science* **2006**, *311*, 829.
(18) Summerscales, O. T.; Cloke, F. G. N.; Hitchcock, P. B.; Green, J. C.; Hazari, N. *J. Am. Chem. Soc.* **2006**, *128*, 9602.
(19) Frey, A. S. P.; Cloke, F. G. N.; Coles, M. P.; Maron, L.; Davin, T. *Angew. Chem., Int. Ed.* **2011**, *50*, 6881.
(20) Castro-Rodriguez, I.; Nakai, H.; Zakharov, L. N.; Rheingold, A. L.; Meyer, K. *Science* **2004**, *305*, 1757.
(21) Castro-Rodriguez, I.; Olsen, K.; Gantzel, P.; Meyer, K. *J. Am. Chem. Soc.* **2003**, *125*, 4565.
(22) Bursten, B. E.; Rhodes, L. F.; Strittmatter, R. J. *J. Am. Chem. Soc.* **1989**, *111*, 2758.
(23) Carmichael, C. D.; Jones, N. A.; Arnold, P. L. *Inorg. Chem.* **2008**, *47*, 8577.
(24) Cloke, F. G. N.; Hawkes, S. A.; Hitchcock, P. B.; Scott, P. *Organometallics* **1994**, *13*, 2895.
(25) Tao, J.; Perdew, J. P.; Staroverov, V. N.; Scuseria, G. E. *Phys. Rev. Lett.* **2003**, *91*, 146401.
(26) Staroverov, V. N.; Scuseria, G. E.; Tao, J.; Perdew, J. P. *J. Chem. Phys.* **2003**, *119*, 12129.
(27) Schäfer, A.; Horn, H.; Ahlrichs, R. *J. Chem. Phys.* **1992**, *97*, 2571.
(28) Furche, F.; Perdew, J. P. *J. Chem. Phys.* **2006**, *124*, 044103(1).
(29) Waller, M. P.; Braun, H.; Hojdis, N.; Buhl, M. *J. Chem. Theory Comput.* **2007**, *3*, 2234.
(30) Fang, M.; Bates, J. E.; Lorenz, S. E.; Lee, D. S.; Rego, D. B.; Ziller, J. W.; Furche, F.; Evans, W. J. *Inorg. Chem.* **2011**, *50*, 1459.
(31) Andrae, D.; Haussermann, U.; Dolg, M. *Theor. Chim. Acta* **1990**, *77*, 123.
(32) Treutler, O.; Ahlrichs, R. *J. Chem. Phys.* **1995**, *102*, 346.
(33) Sierka, M.; Hogekamp, A.; Ahlrichs, R. *J. Chem. Phys.* **2003**, *118*, 9136.
(34) Deglmann, P.; Furche, F.; Ahlrichs, R. *Chem. Phys. Lett.* **2002**, *362*, 511.
(35) Casely, I. J.; Ziller, J. W.; Fang, M.; Furche, F.; Evans, W. J. *J. Am. Chem. Soc.* **2011**, *133*, 5244.
(36) Reed, A. E.; Weinstock, R. B.; Weinhold, F. *J. Chem. Phys.* **1985**, *83*, 735.
(37) Weigend, F.; Ahlrichs, R. *Phys. Chem. Chem. Phys.* **2005**, *18*, 3297.
(38) *TURBOMOLE*, V6−3; TURBOMOLE GmbH: Karlsruhe, 2011; http://www.turbomole.com.
(39) Siladke, N. A.; Ziller, J. W.; Evans, W. J. *Z. Anorg. Allg. Chem.* **2010**, *636*, 2347.
(40) Evans, W. J.; Kozimor, S. A.; Ziller, J. W. *J. Am. Chem. Soc.* **2003**, *125*, 14264.
(41) Evans, W. J.; Miller, K. A.; Ziller, J. W.; Greaves, J. *Inorg. Chem.* **2007**, 46.
(42) Cotton, F. A.; Wilkinson, G.; Murillo, C. A.; Bochmann, M. *Advanced Inorganic Chemistry*, 6th ed.; John Wiley & Sons, Inc.: New York, 1999.
(43) Richter-Addo, G. B.; Legzdins, P. *Metal Nitrosyls*; Oxford University Press: New York, 1992.
(44) Jantunen, K. C.; Burns, C. J.; Castro-Rodriguez, I.; Da Re, R. E.; Golden, J. T.; Morris, D. E.; Scott, B. L.; Taw, F. L.; Kiplinger, J. L. *Organometallics* **2004**, *23*, 4682.
(45) Stewart, J. L.; Andersen, R. A. *Polyhedron* **1998**, *17*, 953.
(46) Diaconescu, P. L.; Cummins, C. C. *J. Am. Chem. Soc.* **2002**, *124*, 7660.
(47) Evans, W. J.; Nyce, G. W.; Forrestal, K. J.; Ziller, J. W. *Organometallics* **2002**, *21*, 1050.
(48) Evans, W. J.; Kozimor, S. A.; Ziller, J. W.; Kaltsoyannis, N. *J. Am. Chem. Soc.* **2004**, *126*, 14533.
(49) Evans, W. J.; Lee, D. S.; Rego, D. B.; Perotti, J. M.; Kozimor, S. A.; Moore, E. K.; Ziller, J. W. *J. Am. Chem. Soc.* **2004**, *126*, 14574.
(50) Arney, D. S. J.; Burns, C. J. *J. Am. Chem. Soc.* **1995**, *117*, 9448.
(51) Cantat, T.; Graves, C. R.; Scott, B. L.; Kiplinger, J. L. *Angew. Chem., Int. Ed.* **2009**, *48*, 3681.
(52) Graves, C. R.; Yang, P.; Kozimor, S. A.; Vaughn, A. E.; Clark, D. L.; Conradson, S. D.; Schelter, E. J.; Scott, B. L.; Thompson, J. D.; Hay, P. J.; Morris, D. E.; Kiplinger, J. L. *J. Am. Chem. Soc.* **2008**, *130*, 5272.
(53) Zi, G.; Jia, L.; Werkema, E. L.; Walter, M. D.; Gottfriedsen, J. P.; Andersen, R. A. *Organometallics* **2005**, *24*, 4251.
(54) Morris, D. E.; Da Re, R. E.; Jantunen, K. C.; Castro-Rodriguez, I.; Kiplinger, J. L. *Organometallics* **2004**, *23*, 5142.
(55) Evans, W. J.; Kozimor, S. A.; Ziller, J. W. *Organometallics* **2005**, *24*, 3407.
(56) Naklicki, M. L.; White, C. A.; Plante, L. L.; Evans, C. E. B.; Crutchley, R. J. *Inorg. Chem.* **1998**, *37*, 1880.
(57) Lam, O. P.; Anthon, C.; Heinemann, F. W.; O'Connor, J. M.; Meyer, K. *J. Am. Chem. Soc.* **2008**, *130*, 6567.
(58) Castro-Rodriguez, I.; Meyer, K. *Chem. Commun.* **2006**, 1353.
(59) Kraft, S. J.; Williams, U. J.; Daly, S. R.; Schelter, E. J.; Kozimor, S. A.; Boland, K. S.; Kikkawa, J. M.; Forrest, W. P.; Christensen, C. N.; Schwarz, D. E.; Fanwick, P. E.; Clark, D. L.; Conradson, S. D.; Bart, S. C. *Inorg. Chem.* **2011**, *50*, 9838.
(60) Dunbar, K. R.; Schelter, E. J.; Palii, A. V.; Ostrovsky, S. M.; Mirovitskii, W. Y.; Hudson, J. M.; Omary, M. A.; Klokishner, S. I.; Tsukerblat, B. S. *J. Phys. Chem. A.* **2003**, *107*, 11102.
(61) Lane, C. B.; Venanzi, L. M. *Inorg. Chim. Acta* **1969**, *3*, 239.
(62) Hirose, M.; Miyake, C.; Du Preez, J. G. H.; Zeelie, B. *Inorg. Chem. Acta* **1988**, *150*, 293.
(63) Huber, K. P.; Herzberg, G. *Constants of Diatomic Molecules* (data prepared by Gallagher, J. W.; Johnson, R. D., III); In NIST Chemistry WebBook, NIST Standard Reference Database Number 69; Linstrom, P. J.,; Mallard, W. G., Eds.; National Institute of Standards and Technology: Gaithersburg MD, 2011; 20899, http://webbook.nist.gov (June 13, 2011).